

A Low-Power High-Sensitivity Analog Front-End for PPG Sensor

Binghui Lin¹, Mohamed Atef², Senior Member, IEEE, and Guoxing Wang³, Senior Member, IEEE

(^{1,2,3}) School of Microelectronics, Shanghai Jiao Tong University, Shanghai, China

(^{1,2,3}) Key Laboratory of Shanghai Education Commission for Intelligent Interaction and Cognitive Engineering

(^{1,2,3}) Brain Science and Technology Research Center, Shanghai Jiao Tong University

(²) Electrical Engineering Department, Assiut University, Assiut, Egypt

(³) guoxing@sjtu.edu.cn

Abstract— This paper presents a low-power analog front-end (AFE) photoplethysmography (PPG) sensor fabricated in 0.35 μm CMOS process. The AFE amplifies the weak photocurrent from the photodiode (PD) and converts it to a strong voltage at the output. In order to decrease the power consumption, the circuits are designed in subthreshold region; so the total biasing current of the AFE is 10 μA . Since the large input DC photocurrent is a big issue for the PPG sensing circuit, we apply a DC photocurrent rejection technique by adding a DC current-cancellation loop to reject the large DC photocurrent up to 10 μA . In addition, a pseudo resistor is used to reduce the high-pass corner frequency below 0.5 Hz and Gm-C filter is adapted to reject the out-of-band noise higher than 16 Hz. For the whole sensor, the amplifier chain can achieve a total gain of 140 dBQ and an input integrated noise current of 68.87 pA_{rms} up to 16 Hz.

I. INTRODUCTION

Photoplethysmography (PPG) signal is used as a measure for the volume changes in blood vessels. Blood pressure (BP) and heart rate are estimated according to the extracted features of the PPG signal [1], [2]. Generally, PPG signal can be measured by transmitted or reflected modes. The LED emits the light which transmits through the tissues and blood vessels of fingers, forehead, wrist and so on. The absorbed light is then modulated by the change in the blood volume. The PPG photocurrent is generated based on light intensity sensed by photodiode (PD) from transmission or reflection path. It is finally amplified and converted to strong voltage signals by a transimpedance amplifier (TIA).

During the last few years, many PPG sensors have been developed, and different research problems have been addressed [3]–[11]. The strength of the PPG signal varies a lot, so a variable gain is necessary [6], [8]–[10]. Motion artifacts (MA) is also an important obstacle; as PPG signal would be affected by human motion or even breathing [8]. Digital signal processing techniques deal with MA noise in [13]–[15], while the work in [10] uses an analog block for MA noise cancellation. The AC to DC ratio of the photocurrent is quite small which is about 1% if red light source is used. As a result, the large DC current may saturate the TIA, which limits the dynamic range of the sensor. Much effort was spent to solve this problem by adding DC photocurrent cancellation loops [3], [4], [7], [9]. Other designs use a DAC for DC current cancellation [5], [6], [8], [10]. Since the useful PPG signal is from 0.5 Hz to 8 Hz, a band-pass system is needed to reject the

out-of-band noise, which requires large resistors and capacitors to achieve the low-pass corner frequency. Some designs, such as [5], [7], used off-chip capacitors to realize it, while [6] designed a low pass filter using switched-capacitor (SC-LPF), and current steering technique to build a LPF was adopted in [7], [9]. Another issue is the required low power operation for the PPG sensor portability. Actually, most of the power consumption is from the LED because the static current of an LED is around several milliamperes while that of the sensor is only several hundred microamperes. Therefore, most of the researches, such as [6], [8], [11], control the duty cycle of the LED so as to reduce its average power. This can make the power consumption of the LED comparable to that of the AFE.

In order to develop a 24-hour wearable healthcare monitoring system, we need sensors, PPG AFE, electroencephalograph (EEG), electrocardiograph (ECG), etc., ADCs, a digital block and radio frequency (RF) circuit for communication as shown in Fig. 1. Besides, low power is required to extend the battery life. The low-noise feature will enable the sensor to sense smaller optical power from LED, so a lower LED power can be further achieved. Then the photon shot noise will become the limitation of the sensitivity of the sensor instead of the noise from the circuit.

This paper introduces a low-power and low-noise integrated PPG sensor with a large dynamic range. The rest part of the paper is organized as follow: Section II presents the architecture of the circuit, Section III shows the simulation results and the last Section IV is the conclusion.

II. THE PROPOSED PPG SENSOR AFE

As shown in Fig. 2, the proposed AFE includes four stages, TIA, post amplifier (PA), Gm-C filter, and buffer. TIA and PA provide the required large gain and small high-pass corner frequency (< 0.5 Hz), while Gm-C LPF filters the out-of-band noise. The last stage is a unity gain buffer to increase the driving ability for the output load.

A. The Proposed TIA Topology

As the first stage of the system, the TIA is used to amplify and convert the weak photocurrent to a strong voltage signal. R_{p1} and R_{p2} are both pseudo resistors which can provide a large resistance of hundreds of giga ohms, shown in Fig. 2. A_1 is the

*This research was supported by the Natural Science Foundation of China under Grant 61474074 and China National 973 Program under Grant 2013CB329401.

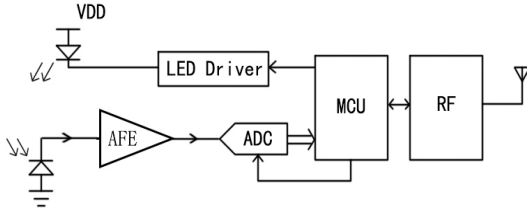


Figure 1. The PPG signal monitoring system.

voltage gain of the core amplifier (OTA_1) and R_f is the shunt feedback resistor. The TIA transimpedance gain is calculated as:

$$A_{TIA} = \frac{-A_1 R_f}{1+A_1} \approx -R_f. \quad (1)$$

C_f works as a compensation capacitor.

In order to cancel the large input DC photocurrent, the DC current rejection technique is used by adding a feedback loop with an error amplifier (EA) (shown in Fig. 2), which has been risen up in [7]. When the DC photocurrent is zero, both the DC voltages of the TIA output and its negative input node are equal to V_{ref} , which makes the output voltage of EA high enough to turn off M_{ctrl} . When the DC photocurrent gets higher, the output voltage of the TIA will be higher than V_{ref} and EA will generate a low output voltage which can turn on M_{ctrl} . As a result, the PD DC current passes through M_{ctrl} , which prevents the DC photocurrent from passing through R_f and keeps TIA away from saturation. However, this loop is a negative feedback so it may feed part of the AC PPG signal back and lower the transimpedance gain. To solve this problem, a low-pass network in the feedback loop is necessary to stop the PPG signal from passing through the loop. Since the high-pass corner frequency is much lower than 0.5 Hz, C_C between the input and output node of EA is used to get large capacitance due to Miller Effect. The transfer function of the TIA can be calculated by

$$Z_{TIA}(s) = -R_f \frac{1+sC_C R_{p2}(1+A_{v,EA})}{1+sC_C R_{p2}(1+A_{v,EA})+R_f g_{m,ctrl} A_{v,EA}}. \quad (2)$$

$A_{v,EA}$ is the gain of EA and $g_{m,ctrl}$ is the transconductance of M_{ctrl} in (2). Practically $A_{v,EA}$ is much bigger than one so (2) can be approximated as

$$Z_{TIA}(s) \approx -R_f \frac{1+sC_C R_{p2} A_{v,EA}}{1+sC_C R_{p2} A_{v,EA}+R_f g_{m,ctrl} A_{v,EA}}. \quad (3)$$

From (3), it is indicated that this TIA is high pass so the feedback loop hardly lowers the transimpedance gain of TIA. There is a zero and a pole as shown in (4) and (5).

$$\omega_z(s) = \frac{1}{C_C R_{p2} A_{v,EA}}. \quad (4)$$

$$\omega_p(s) = \frac{1+R_f g_{m,ctrl} A_{v,EA}}{C_C R_{p2} A_{v,EA}}. \quad (5)$$

In our circuit, R_f , C_f and C_C is $1.255 \text{ M}\Omega$, 8.68 pF and 65.091 pF respectively so the transimpedance gain of TIA is about $122 \text{ dB}\Omega$ and high-pass corner frequency is below 0.5 Hz due to the pseudo resistor with the current consumption of $6.575 \mu\text{A}$.

The core amplifier of the TIA is OTA_1 which is a two-stage operational transconductance amplifier (OTA) shown in Fig. 3. M_1 and M_2 are the input stage with active load of M_3 and M_4

while M_{SS} is the current source providing a small bias current. They are all working in subthreshold region for power reduction issue. M_5 and M_6 are the output stage whose current should be large enough, about $2 \mu\text{A}$, to handle the remaining DC photocurrent from PD after rejection. R_Z and C_C are used for compensation. For typical corner, our design can reject the DC photocurrent that is up to $10 \mu\text{A}$. The simulation result of TIA's frequency response is shown in Fig. 4 when the DC photocurrent is from 50 nA to $10 \mu\text{A}$. The integrated noise of TIA is $347.8 \text{ pA}_{\text{rms}}$.

B. Capacitive Post Amplifier

It is a voltage amplifier with the gain of C_1/C_2 . Due to C_1 , only AC signal is coupled to the second stage so the variation of the DC photocurrent has no effect on the following stages. The transfer function is approximately

$$H_2(s) \approx -\frac{sC_1 R_{p3}}{1+sC_2 R_{p3}} \quad (6)$$

In our design, C_1/C_2 is 10 and C_2 is 2.1 pF , which can achieve a gain of 20 dB at 507.6 nA biasing current.

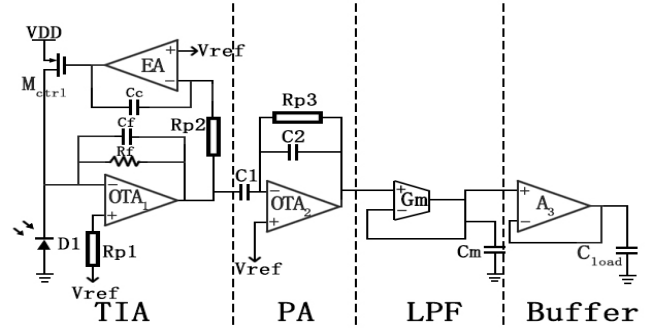


Figure 2. The AFE block diagram.

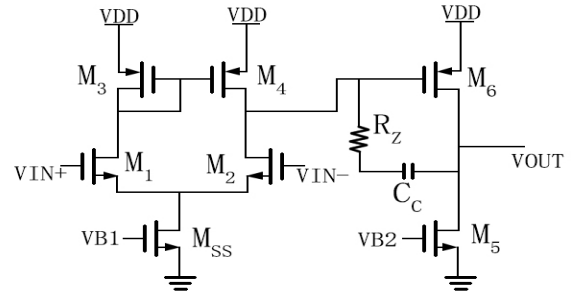


Figure 3. Schematic of OTA_1 used with the proposed TIA.

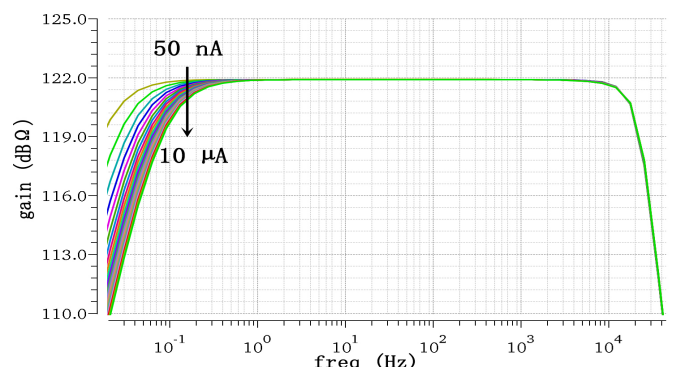


Figure 4. Frequency response of TIA with different DC photocurrent inputs from 50 nA to $10 \mu\text{A}$.

C. Gm-C Low-pass Filter

Since the useful bandwidth of PPG signal is 8 Hz, a low-pass filter is needed for out-of-band noise rejection. The difficulty for the filter design is to achieve a very low corner frequency. Thus, some techniques have been developed, such as SC-LPF [6], current steering technique [7], [9] and Gm-C filter [12]. SC-LPF needs a complex digital control block and current steering technique needs accurate bias voltages. As for Gm-C filter, such as the one in our circuit, the transfer function $H_3(s)$ is calculated as:

$$H_3(s) = \frac{1}{1+s\frac{C_m}{G_m}} \quad (7)$$

The pole is G_m/C_m so it is needed to make a small G_m . By making a trade-off between reliability and complexity of the circuit, the Series-Parallel (SP) Architecture in [12] is used to build the Gm block. M_2 is the current mirror. M_{2A} and M_{2C} are made up by N MOSFETs in parallel in order to increase the width while M_{2B} and M_{2D} are made up by M MOSFETs in series in order to increase the equivalent length. Therefore, the drain current of M_3 is reduced by $M \times N$ times from that of M_1 and the equivalent transconductance is reduced by $M \times N$ times from the input transistor. In order to match these transistors in series and parallel, the common-centroid technique in layout has been applied.

In Fig. 5, M and N are both 20 so the equivalent G_m is equal to $g_{m1}/400$. The bias current is about 80 nA and C_m is 18.63 pF so that the corner frequency is about 20 Hz. For the whole stage, the current consumption is only 178.5 nA.

III. POST LAYOUT SIMULATION RESULTS

The proposed system is implemented in 0.35 μ m CMOS process with a single power supply of 3.3 V. Fig. 6 shows the layout of the whole system. The total size of the chip including pads is 1 mm².

A. AC and Transient Simulation Results at Typical Corner

Since the input DC photocurrent would affect the circuit though we use the robust DC photocurrent rejection technique, AC and transient simulation with different DC current input should be observed. Fig. 7 shows the frequency response of the whole circuit when the input DC current increases from 0 to 10 μ A. It is obvious that the pass band covers the range from 0.5 Hz to 8 Hz so the PPG signal can pass through this system with the gain of about 142 dB Ω . Fig. 8 shows the transient outputs with the PPG input signals (AC) whose amplitude are 1 nA and 100 nA. For each case, the DC level is 100 times as the AC amplitude. The DC rejection circuit successfully rejects the large DC photocurrent.

B. PVT Post Layout Simulation Results

The PVT post layout simulation at different process corners with the supply voltage varied from 3 V to 3.3 V and the temperature varied from 10 °C to 50 °C is performed. There is no need for a wider temperature range because the circuit which contacts with human body should be warm. Table I shows the simulation result of input referred noise with DC input current of 100 nA and the corner frequencies of the whole circuit. It is indicated that the pass band of the system is from 88.26 mHz to 16.19 Hz with the transimpedance gain of at least 139 dB Ω . Besides, the worst current consumption is

11.66 μ A. Comparing with the noise of TIA, the integrated noise of the whole system is reduced dramatically to 68.87 pA_{rms} because of the on-chip LPF. Due to the variation of the Gm-C filter's bias current, high corner frequency varies from 16.19 Hz to 43.67 Hz. It is not accurate enough for a LPF but it is bearable for our application.

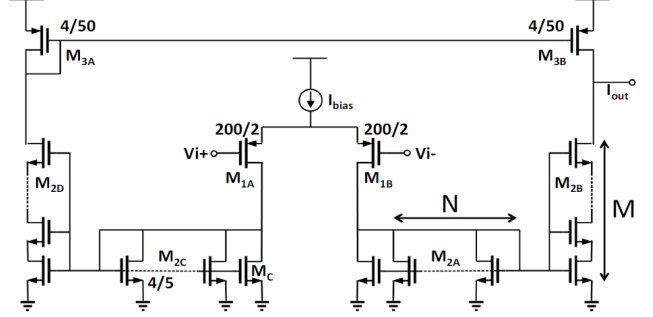


Figure 5. Schematic of Gm block [12].

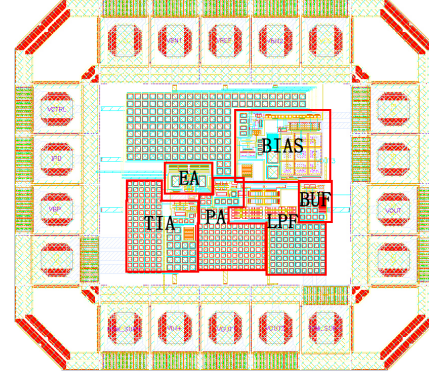


Figure 6. Layout of the whole system.

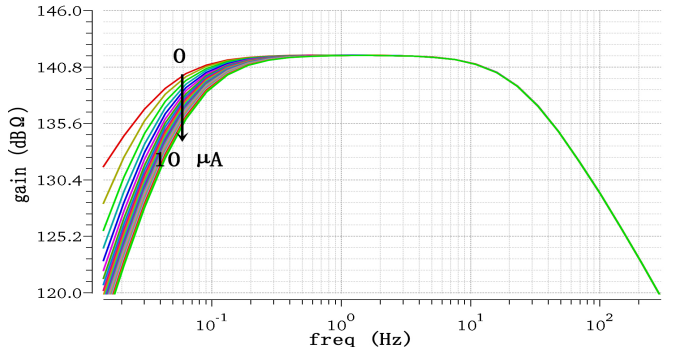


Figure 7. Frequency response with different DC photocurrent inputs from 0 to 10 μ A.

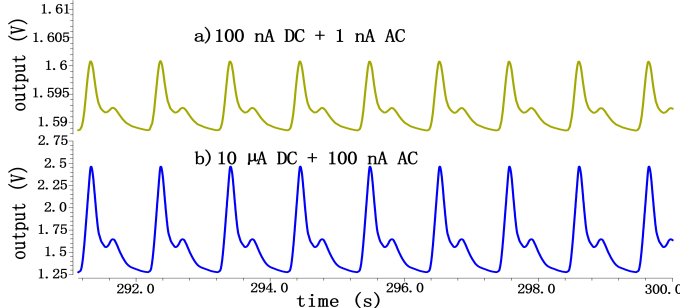


Figure 8. Transient response with a) 1 nA and b) 100 nA input signal.

C. Monte Carlo Simulation Results

Monte Carlo post layout simulation is employed to study the impact of process variation on the performance of the proposed system. As is shown in Fig. 9, the transimpedance gain, low and high corner frequency and static current are calculated for 1000 runs with a DC input of 10 μ A. The figure indicates the mean value and standard deviation of each parameter.

D. Performance Summary and Comparison

Table II is the performance of the proposed AFE and the comparison with other PPG sensors published in recent years. It is indicated that our design has very low current consumption and noise with wide dynamic range.

IV. CONCLUSION

The low-power operation for the proposed integrated PPG

TABLE I. PVT RESULT FOR VDD FROM 3 V TO 3.3 V AND TEMPERATURE FROM 10 °C TO 50 °C.

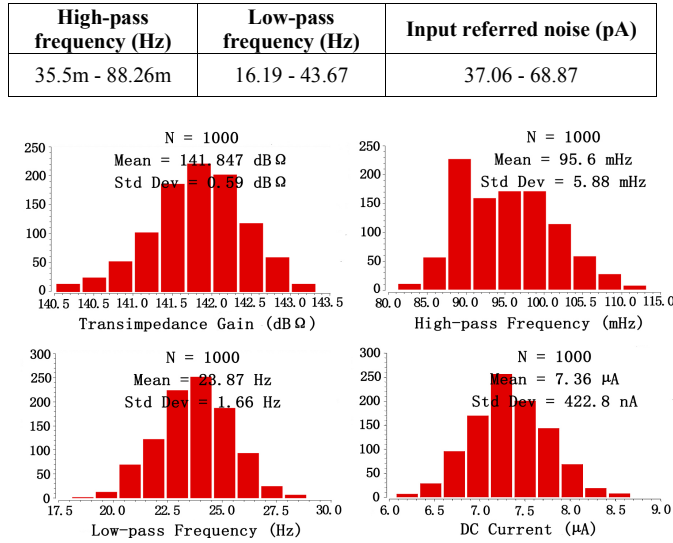


Figure 9. Monte Carlo simulation results.

TABLE II. COMPARISON WITH RECENTLY PUBLISHED PPG SENSORS

Design	[3]	[4]	[5]	[6]	[10]	This work
Process (um)	0.35	0.13	0.18	0.18	0.13	0.35
V_{DD} (V)	2.5	1.2	3.3	1.2	1.2	3.3
Gain (dBΩ)	63.5	89	60	-----	130.9	139
High-pass frequency (Hz)	0.5	0.5	0.2	0.5	0.1	95.6m
Low-pass frequency (Hz)	N/A	N/A	20	3.5	70	16.19
Input referred noise (nA)	40.8	-----	1.8	0.486	0.26	0.0689
Power consumption (uW)	145	55.7	1502	172	26.4	38
DC rejection current (uA)	15	85	1.25	10	30	10
Monolithic	yes	yes	no	yes	-----	yes

sensor AFE is achieved using the subthreshold operation for all the circuitries. The high-sensitivity TIA in conjunction with the 16.19 Hz Gm-C low-pass filter reduces the AFE total noise to 68.9 pA. Both the adopted DC photocurrent cancellation loop and the achieved low noise extend the dynamic range of the AFE. The proposed AFE PPG sensor performance enables it to be a good candidate for a long-term wearable healthcare monitoring device.

REFERENCES

- [1] K. W. Chan, K. Hung and Y. T. Zhang, "Noninvasive and Cuffless Measurements of Blood Pressure for Telemedicine," IEEE Proc. EMBS Conf., Istanbul, Turkey, Vol. 4, 2001, pp. 3592–3593.
- [2] J. D. Bronzino, The Biomedical Engineering Handbook, Boca Raton, FL: CRC Press, 2000.
- [3] A. K. Y. Wong, K. N. Leung, K. P. Pun and Y. T. Zhang, "A 0.5-Hz High-Pass Cutoff Dual-Loop Transimpedance Amplifier for Wearable NIR Sensing Device," IEEE Transactions on Circuits and Systems II: Express Briefs, vol. 57, no. 7, pp. 531-535, July 2010.
- [4] Y. Li, A. K. Y. Wong and Y. T. Zhang, "Fully-Integrated Transimpedance Amplifier for Photoplethysmographic Signal Processing with Two-Stage Miller Capacitance Multiplier," Electronics Letters, vol. 46, no. 11, pp. 745-746, May 2010.
- [5] SS. Cheng, SC. Huang, TH. Tran et al. "A 1.5 mW Front-End Readout Circuit for a Small-Sized Melanin Sensor," Microsyst Technol (2016) 22: 1449.
- [6] P. V. Rajesh et al., "A 172uW Compressive Sampling Photoplethysmographic Readout with Embedded Direct Heart-rate and Variability Extraction from Compressively Sampled Data," 2016 IEEE International Solid-State Circuits Conference, San Francisco, CA, 2016, pp. 386-387.
- [7] A. K. Y. Wong, K. P. Pun, Y. T. Zhang and K. N. Leung, "A Low-Power CMOS Front-End for Photoplethysmographic Signal Acquisition With Robust DC Photocurrent Rejection," IEEE Transactions on Biomedical Circuits and Systems, vol. 2, no. 4, pp. 280-288, Dec. 2008.
- [8] M. Konijnenburg et al., "A Multi(bio)sensor Acquisition System With Integrated Processor, Power Management, 8 × 8 LED Drivers, and Simultaneously Synchronized ECG, BIO-Z, GSR, and Two PPG Readouts," IEEE Journal of Solid-State Circuits, vol. 51, no. 11, pp. 2584-2595, Nov. 2016.
- [9] A. Wong, Kong-Pang Pun, Yuan-Ting Zhang and K. Hung, "A Near-Infrared Heart Rate Measurement IC with Very Low Cutoff Frequency Using Current Steering Technique," IEEE Transactions on Circuits and Systems I: Regular Papers, vol. 52, no. 12, pp. 2642-2647, Dec. 2005.
- [10] J. Kim, J. Kim, and H. Ko, "Low-Power Photoplethysmogram Acquisition Integrated Circuit with Robust Light Interference Compensation," Sensors, vol. 16, no. 1, pp. 46, Dec. 2015.
- [11] I. Kim, R. Lobo, J. Homer and Y. A. Bhagat, "Multimodal Analog Front-End for Wearable Bio-Sensors," 2015 IEEE Sensors, Busan, 2015, pp. 1-4.
- [12] Y. C. Lee, W. Y. Hsu, T. T. Huang and H. Chen, "A compact Gm-C Filter Architecture with an Ultra-Low Corner Frequency and High Ground-Noise Rejection," 2013 IEEE Biomedical Circuits and Systems Conference, Rotterdam, 2013, pp. 318-321.
- [13] M. Raghu Ram, K. Venu Madhav, E. Hari Krishna, Nagarjuna Reddy Komalla, and K. Ashoka Reddy, "A Novel Approach for Motion Artifact Reduction in PPG Signals Based on AS-LMS Adaptive Filter," IEEE Transactions on Instrumentation and Measurement, vol. 61, no. 5, pp. 1445-1457, 2012.
- [14] Ming-Zher Poh, Nicholas C. Swenson and Rosalind W. Picard, "Motion-Tolerant Magnetic Earring Sensor and Wireless Earpiece for Wearable Photoplethysmography," IEEE Transactions on Information Technology in Biomedicine, vol. 14, no. 3, pp. 786-794, 2010.
- [15] Takunori Shimazaki, Shinsuke Hara, "Breathing Motion Artifact Cancellation in PPG-Based Heart Rate Sensing," 9th International Symposium on Medical Information and Communication Technology, pp. 200-203, 2015.